

Melting of pseudopotential sodium from molecular dynamics

Brad L. Holian, Galen K. Straub, Richard E. Swanson,* and Duane C. Wallace

Los Alamos National Laboratory, Los Alamos, New Mexico, 87545

(Received 10 August 1982)

For a pseudopotential model of metallic sodium, the Gibbs free energy of the fluid phase was calculated by a combination of molecular dynamics and the high-temperature free-energy expansion. From these calculations, together with previous molecular-dynamics results for crystalline sodium, the melting transition was determined as a function of pressure, up to 16 kbar. The pressure-temperature phase line is in good agreement with experiment, and so are the changes associated with melting at zero pressure, namely the heat of fusion, the entropy of fusion, and the relative volume change. The dynamic melting process, previously observed in molecular-dynamics simulations of sodium, is also in good agreement with the present equilibrium calculations.

I. INTRODUCTION

We have previously reported the results of lattice-dynamics and molecular-dynamics calculations for pseudopotential sodium in the solid phase.^{1,2} It was concluded that a simple yet accurate way to represent the thermodynamic properties of sodium, and presumably of all crystalline solids except for quantum crystals, is to use quasiharmonic lattice dynamics in the quantum regime and molecular dynamics in the classical regime. In this way anharmonic effects are partially included at low temperatures, through the volume dependence of the phonon frequencies, and anharmonic effects are completely included at high temperatures, within the accuracy of classical statistics. In this paper we report on molecular-dynamics calculations of the melting of pseudopotential sodium, at modest pressures ranging from 0 to 16 kbar. The molecular-dynamics method is appropriate for this problem, because the motion of the sodium ions in the solid and fluid phases near melting is essentially classical.

In order to construct the equilibrium melting line, the free energies of the solid and fluid phases must be computed, and this requires a separate determination of the entropy constant for each phase. In our study of solid sodium, we assumed the classical anharmonic free energy could be represented as a power series in the temperature T , of lowest order T^2 , so that the classical anharmonic entropy has no constant term; then the classical entropy constant is given by the quasiharmonic high-temperature limit. For the fluid, we can use the high-temperature cluster expansion of the free energy, appropriate for a metal fluid.³ The cluster expansion, and determination of the equilibrium melting line for pseudopotential sodium, are discussed in Sec. II. Our

molecular-dynamics systems also exhibit dynamic melting, in which the crystalline phase, upon heating to a certain temperature or above, loses its long-range order and gives way to a fluid phase. The calculated melting properties, both equilibrium and dynamic, and the experimental melting properties are compared in Sec. III.

II. CALCULATION OF EQUILIBRIUM MELTING

It is necessary at the outset to establish notation and recall some needed equations. There are N atoms in a volume V , and the volume per atom is $v = V/N$. We adopt the practice of normalizing energies to a per atom basis, which corresponds to setting $N = 1$ in the usual equations.^{1,2} In pseudopotential perturbation theory, the potential energy Φ of the metal fluid is given by

$$\Phi - I_z = \Omega(v) + \sum \phi(r;v), \quad (1)$$

where I_z is the ionization energy, $\Omega(v)$ is a volume-dependent binding potential, $\phi(r;v)$ is a central potential between two ions separated by a distance r , and the sum is over all distinct pairs of ions. Equations for Ω and ϕ , in a form convenient for molecular-dynamics calculations, were given previously.² The high-temperature cluster expansions of the thermodynamic functions³ are also needed. Corresponding to the thermodynamic internal energy U , we define a reduced function U^* whose high-temperature expansion is (k is the Boltzmann's constant)

$$U^* = \frac{U - I_z - \Omega}{kT} = \frac{3}{2} - \frac{T}{v} \frac{\partial B_2}{\partial T} + \dots \quad (2)$$

Here B_2 is the second virial coefficient,

$$B_2(T, v) = 2\pi \int_0^\infty \{1 - \exp[-\phi(r; v)/kT]\} r^2 dr, \quad (3)$$

and the ellipsis in Eq. (2) represents terms in higher virial coefficients. Similar expansions for the pressure P and the Helmholtz free energy F are

$$P^* = \frac{Pv + d\Omega/d \ln v}{kT} = 1 + \left[\frac{B_2}{v} - \frac{\partial B_2}{\partial v} \right] + \dots, \quad (4)$$

$$F^* = \frac{F - I_z - \Omega}{kT} = \ln \left[\frac{\Lambda^3}{v} \right] - 1 + \frac{B_2}{v} + \dots, \quad (5)$$

where Λ is the thermal de Broglie wavelength, given in terms of the ion mass M by $\Lambda^2 = 2\pi\hbar^2/MkT$.

We are now ready to describe our calculation of the free energy for fluid sodium in the region near melting. The first step is to evaluate the constant of integration in the entropy of the fluid phase. This can be done by evaluating the expansion (5) for F^* at a temperature sufficiently high so that the expansion converges; further, to simplify this evaluation, the temperature should be high enough to make the convergence of (5) extremely rapid. Since the terms beyond B_2 in (5) are difficult to compute, we devised the following method to estimate the convergence of this series. Molecular-dynamics calculations of U and P as functions of T were carried out for the standard volume of $256a_0^3/\text{atom}$. In Table I, the results are compared with the second-order cluster expansions for U^* and P^* . It is seen that the second-order approximations become more accurate as temperature increases, and that they are quite accurate at the highest temperature of 1.160 Ry. The same is presumably true for the function F^* , whose second-

TABLE I. Molecular-dynamics results for U^* and P^* as functions of kT , compared with the second-order cluster-expansion terms, i.e., the terms involving B_2 . All quantities are evaluated at $v = 256a_0^3/\text{atom}$.

kT (Ry)	$U^* - \frac{3}{2}$	$-\frac{T}{v} \frac{\partial B_2}{\partial T}$	$P^* - 1$	$\frac{B_2}{v} - \frac{\partial B_2}{\partial v}$
1.160	0.1269	0.1207	0.1865	0.1801
0.6050	0.1852	0.1670	0.3075	0.2864
0.2269	0.3083	0.2319	0.6389	0.5315
0.09161	0.4478	0.2402	1.222	0.8710
0.04084	0.5490	0.1290	2.179	1.287
0.01100	0.3977		5.815	
0.005721	-0.1964		9.741	

order approximation is given by (5). Further, the third-order contribution to F^* is $B_3/2v^2$, which can be estimated as follows. At $kT = 1.160$ Ry, we assume the difference between molecular dynamics and the second-order approximation for P^* is due entirely to the term in B_3 ; in this term we neglect $\partial B_3/\partial v$ compared to B_3/v , since $\partial B_2/\partial v$ is an order of magnitude smaller than B_2/v at $kT = 1.160$ Ry; this gives us the estimate $B_3/2v^2 = 0.0032$. Then with the value $B_2/v = 0.1675$, we find $F^* = -18.765$ at $kT = 1.160$ Ry ($T = 183\,200$ K).

Additional molecular-dynamics evaluations of U and P for fluid sodium, for the three volumes 232, 256, and $270a_0^3/\text{atom}$ and for temperatures in the range 400–700 K, were reported in Ref. 2. To calculate the free energy at each of these three volumes, we proceed as follows. From the data for U^* at the standard volume, dF^* is integrated numerically from $T = 183\,200$ K down to $T = 500$ K, the differential at constant volume being

$$dF^* = -U^* d \ln T. \quad (6)$$

This gives $F^* = -8.465$ at $T = 500$ K, with an estimated numerical error of not more than ± 0.02 . Then at the fixed temperature of 500 K, dF^* is integrated numerically from the standard volume to the volumes 232 and $270a_0^3/\text{atom}$, where the differential at constant temperature is

$$dF^* = -P^* d \ln v. \quad (7)$$

Finally (6) is used again to compute F^* at each volume for temperatures below 500 K.

It is now possible to solve the conditions for equilibrium melting at a constant temperature T_m and a constant pressure P_m . With the Gibbs function $G = F + Pv$, and subscripts f or s for fluid or solid, respectively, the fluid-solid coexistence equations are

$$P_f(v_f, T_m) = P_s(v_s, T_m) = P_m(T_m) \quad (8)$$

$$G_f(P_m, T_m) = G_s(P_m, T_m). \quad (9)$$

At each fluid volume v_f , these equations were solved for T_m, P_m , and the corresponding solid volume v_s . To reach the melting temperature at each fluid volume, it was necessary to extrapolate the fluid data for U and P downward in temperature. For the solid phase, we used the previously reported data for F and P as functions of v and T .² Results of the melting determinations, including the latent heat of fusion ΔH_m and the entropy of fusion ΔS_m , are listed in Table II.

III. DISCUSSION

Theory and experiment for equilibrium melting are compared in Fig. 1, where the solid circles show

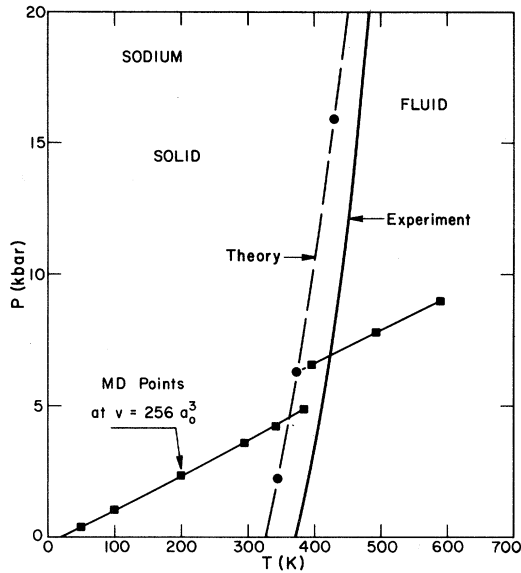


FIG. 1. P - T phase diagram for sodium. Solid line is the experimental melting curve, and solid circles show the calculated equilibrium melting points. The solid squares are molecular-dynamics results for the fixed volume of $256a_0^3$ /atom; dynamic melting takes place between the highest point on the solid-phase branch (385 K) and the lowest point on the fluid-phase branch (396 K). Short dash shows the extrapolation of fluid data needed to reach the equilibrium melting temperature.

our calculated points, and the solid line represents the measurements of Kennedy and co-workers.^{4,5} The theoretical curve lies in the range 30–46 K below the experimental curve. We estimate the following errors in our calculations. First, thermal excitation of conduction electrons gives a small T^2 contribution to the Gibbs function, and if this were included in our theory, the calculated melting temperatures would be lowered by about 0.01 K. Second, molecular dynamics treats the motion of the ions classically, and quantum corrections would change our calculated T_m , but by less than ± 2 K. Finally, numerical error in our construction of the fluid-phase free energy, say $\pm 0.02kT$, could alter

our calculated melting temperatures by ± 10 K. Hence the discrepancy between theory and experiment for the melting curve cannot be covered by the above sources of error in the theory. Some error undoubtedly results from the finite size of our molecular-dynamics computational cell (678 atoms in a tetragonal box; see Ref. 2), but at the present time we believe this error is quite small. The most likely cause of the discrepancy is some small imperfection in our pseudopotential model for the potentials in sodium; many possibilities could be cited, including that of a small change in the electronic structure between the solid and fluid phases. From the point of view of an overall evaluation of the theory, however, the observed theoretical-experimental difference is trivial. Indeed, it is remarkable that such a simple theory as we have described can yield an equilibrium solid-fluid phase boundary within approximately 10% of experiment.

Calculated and measured values are compared in Table III for several properties of the melting transition at zero pressure. The theory is 12% low for the melting temperature and for the latent heat of fusion, while theoretical results for the entropy of fusion and the volume change on melting are in excellent agreement with experiment. In Table III, the range of experimental values of the initial slope dT_m/dP_m of the melting line represents the variation in measured results.^{4–6} The value corresponding to Martin's heat of fusion⁷ and to $\Delta v/v=0.025$ is $dT_m/dP_m=8.8$ K/kbar, which is close to our calculated result.

Another characteristic of our molecular-dynamics simulations is the process of dynamic melting,² which occurs as follows. Each molecular-dynamics computation was started with the atoms located at bcc lattice sites, and with a distribution of velocities. When the initial total kinetic energy was not too large the system equilibrated in the crystalline phase at some temperature; when the initial kinetic energy was above a certain threshold, the system came to equilibrium in the fluid phase, at a temperature above the dynamic melting temperature. The situation is illustrated in Fig. 1, where the solid squares

TABLE II. Equilibrium melting solutions from molecular dynamics for pseudopotential sodium. The zero-pressure values were obtained by extrapolation.

v_f (a_0^3 /atom)	T_m (K)	P_m (kbar)	ΔH_m (cal/mole)	$\Delta S_m/k$	$\frac{v_v - v_s}{v_f}$
232	430.4	15.93	707	0.827	0.017
256	373.5	6.27	622	0.838	0.020
270	345.2	2.26	577	0.841	0.022
279	327.0	0	548	0.844	0.024

TABLE III. Zero-pressure melting data from molecular-dynamics (MD) calculations of pseudopotential sodium compared with experiment.

	T_m (K)	V_f (cm ³ /mole)	ΔH_m (cal/mole)	$\Delta S_m/k$	$\frac{V_f - V_s}{V_v}$	dT_m/dP_m (K/kbar)
MD	327	24.9	548	0.84	0.024	8.6
Expt.	371 ^a	24.8	621 ^a	0.84	0.025	8.5–11.7 ^b

^a Reference 7.

^b References 4–6.

show the molecular-dynamics results for $P(T)$ at the standard volume of $256a_0^3/\text{atom}$. The points fall on two distinct curves, corresponding to solid and fluid phases. The highest temperature on the solid branch is 385 K, the lowest temperature on the fluid branch is 396 K, and constant-volume melting presumably takes place in the intervening region. We cannot plot points in this intervening region, because the molecular-dynamics system does not reach a stable

equilibrium here. For constant-pressure melting at the fluid volume of $256a_0^3/\text{atom}$, the dynamic melting temperature is close to 396 K, which is about 22 K higher than the corresponding equilibrium melting temperature. We believe the dynamic melting process is sensitive to the molecular-dynamics cell size, more so than equilibrium melting, and for very large cells we expect the dynamic melting temperature to approach the equilibrium value.

*Present address: U.S. Air Force Academy, Colorado 80840.

¹D. C. Wallace, Phys. Rev. **176**, 832 (1968).

²R. E. Swanson, G. K. Straub, B. L. Holian, and D. C. Wallace, Phys. Rev. B **25**, 7807 (1982).

³D. C. Wallace, B. L. Holian, J. D. Johnson, and G. K. Straub, Phys. Rev. A **26**, 2882 (1982).

⁴P. W. Mirwald and G. C. Kennedy, J. Phys. Chem. Solids **37**, 795 (1976).

⁵H. D. Luedemann and G. C. Kennedy, J. Geophys. Res. **73**, 2795 (1968).

⁶V. A. Ivanov, I. N. Makarenko, A. M. Nikolaenko, and S. M. Stishov, Phys. Lett. **47A**, 75 (1974).

⁷D. L. Martin, Phys. Rev. **154**, 571 (1967).